Earthquake Engineering, Tenth World Conference © 1992 Balkema, Rotterdam. ISBN 90 5410 060 5

Effective repair with resin for bond failure of RC members

A.Tasai
Department of Architecture, University of Tokyo, Japan

ABSTRACT: Effect repair method of damaged concrete members reinforced with round or deformed bars was studied experimentally. In specimens using round bars, their cover concrete was replaced by epoxy mortar or pre-packed concrete mixed resin. In specimens using deformed bars, low viscous epoxy resin was injected into bond splitting cracks along main bars. Performance of repaired specimens was better than that of original specimens. Bond resisting mechanisms were studied. Effect of repair depended on high adhesive capacity of resin.

1 INTRODUCTION

Bond failure between concrete and main reinforcement is one of earthquake damage types in reinforced concrete members, which reduces member stiffness considerably. Hence, some repair work or retrofit work must be done to improve bond capacity if the structure is to be used. In this paper, the effect of repair with resin on bond performance is clarified experimentally. Effective repair methods are proposed for round and deformed bar.

2 REPAIR OF BOND ALONG ROUND BARS

Old concrete structures are often reinforced with round bars. Bond failure between concrete and round bars will easily occur during earthquakes because bond resistance along round bars depends on adhesive action of concrete which deteriorates at a low stress level. Effective repair method for this type of failure was studied experimentally. Two materials were used in repair work;i.e., epoxy mortar and prepacked concrete mixed with resin. These materials are expected high adhesive resistance.

2.1 *Testing Program*

Two short column specimens (FR15-1, FR15-2) and two long column specimens (FR25-1, FR25-2) were tested. The shear span to depth ratio was 1.5 in the short columns and 2.5 in the long columns. All specimens had a uniform section of 250 x 250 mm (Fig.1). The main variable was repair methods. The specimens were reinforced by 3-13ϕ(diameter;13 mm, round bars) in tension with a tensile reinforcement ratio of 0.64 percent. The shear reinforcement ratio was 0.15 percent (2-6ϕ@150mm). Steel plates were welded to main bars in the stab near the critical section to aboid slipping out of the bars from the stab.

A specimen was subjected to antisymmetric bending reversals up to 1/30 rad in relative deflection angle

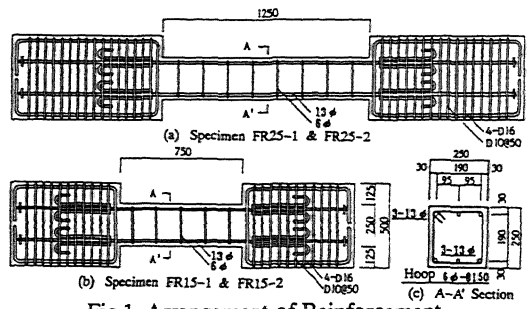

Fig.1 Arrangement of Reinforcement

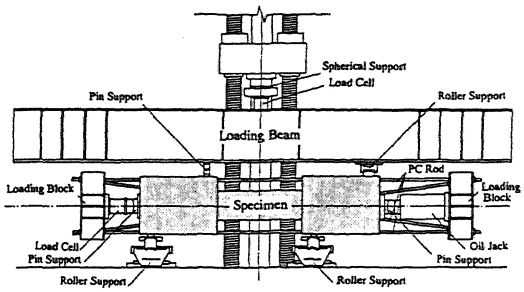

Fig.2 Loading Apparatus.

Table 1 Material Properties

(a) Compressive Strength of Concrete	
Specimen FR15-1, FR25-1	23.7 MPa
Specimen FR15-2, FR25-2	24.6 MPa
(b) Main Reinforcement 13ϕ	
Yield Strength	324 MPa
Yield Strain	0.00168 mm/mm
Strain at Strain Hardening	0.02690 mm/mm
(c) Prepacked Concrete	
Compressive Strength	28.9 MPa
(d) Epoxy Mortar	
Compressive Strength	77.8 MPa
Tensile Strength	30.9 MPa
Elastic Modulus	6480 MPa

between both stabs by a mechanically controlled universal testing machine (Fig.2). Loading direction was reversed by shifting the loading and supporting points. A constant axial load of 300 KN was applied to all specimens. Relative displacement between both stubs was measured by displacement transducers. Strains of the longitudinal reinforcement were measured at every 15-cm by strain gages. Material properties of concrete and reinforcement are listed in Table 1.a,b.

2.2 *Repair Method*

During the original loading, concrete crushed and spalled in the both critical regions of each specimen, but no damage was observed in the mid-span region in all specimens. The damage was repaired by two methods;i.e., (a) replacing crushed concrete by high strength material (specimens FR15-1 and FR25-1), and (b) restoring bond of longitudinal reinforcement, (specimens FR15-2 and FR25-2). The residual deformations due to the original loading of the specimens were corrected before the repair work.

Repair methods of each specimen are illustrated in Fig.3. In specimens FR15-1 and FR25-1, only critical regions were repaired as follows. Crushed or spalled concrete in both ends of the member was removed by a rock drill or a chisel and a hammer. Forms were set around the cavity and then high strength epoxy mortar, epoxy mixed with fine aggregate, was placed to restore the original shape.

Specimen FR15-2 was repaired to restore bond along the longitudinal reinforcement. Crushed concrete in both ends of the member was removed. In addition, all cover along the longitudinal reinforcement was also removed to expose its surface. Forms were set to restore the original shape and then the cavity was filled with dry aggregates. Mixed polymer cement slurry was injected continuously through pipes fitted to the form using a hand-controlled pump. The new concrete is called "prepacked concrete" in this paper.

In specimen FR25-2 with long shear span length, cover concrete of 15 cm long in the mid-span was removed to expose the surface of main bar and replaced by epoxy mortar to improve bond between concrete and main bar. Crushed concrete in both ends of the member were replaced by prepacked concrete.

During the repair work, strain gages located in the exposed part of the longitudinal bar were replaced by new ones in all specimens. Letter R is used to denote the specimen after repair such as RFR15-1, RFR25-1, RFR15-2 and RFR25-2. Material properties of prepacked concrete and epoxy mortar are listed in Table 1.c,d.

2.3 *Test Results*

During the original loading, regardless shear span to depth ratio, flexural or flexural shear cracks occurred in the critical regions of all columns, and then concrete started to crush during a loading cycle at a deflection angle of 1/50 rad, and eventually concrete crushed completely in the final loading cycle. Neither crack nor crush of concrete was observed in the mid-span portion of each column after the original loading.

During the loading after repair, in specimens RFR15-1 and RFR25-1, flexural cracks occurred at the critical section and along the boundary between the replaced epoxy mortar and the original concrete. The width of cracks along the boundary was always larger than that at the critical section. No crush was observed in the replaced epoxy mortar region until the final loading steps. On the contrary, the replaced prepacked concrete at the ends of specimens RFR15-2 and RFR25-2 started to crush during the loading cycle at a deflection angle of 1/50 rad and the final failure mode was similar to that of the original specimens.

Load-deflection relations obtained from the tests before and after repair are shown in Fig.4. Dashed lines and solid lines indicate the results before and after repair, respectively. These relations represent the following obvious characteristic;i.e., the stiffness of specimens RFR15-1 and FR25-1 was considerably lower than that before repair, and the hysteretic areas were significantly smaller than that at the same amplitude in the original loading. On the contrary, the bond repaired specimens RFR15-2 and RFR25-2 developed the same level of stiffness as the virgin specimens and the energy dissipation ability was larger than the virgin specimen. In order to develop good performance after repair, it is important to restore the bond along longitu-

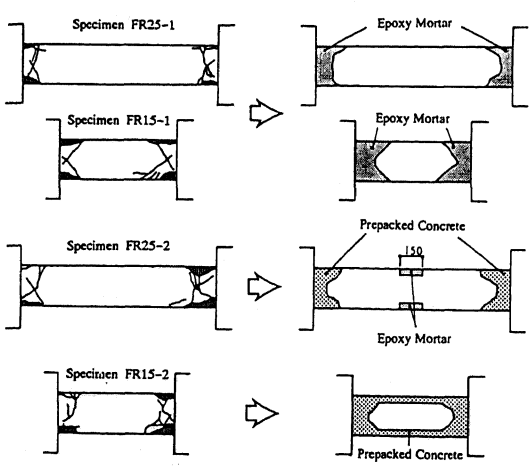

Fig.3 Repair Methods

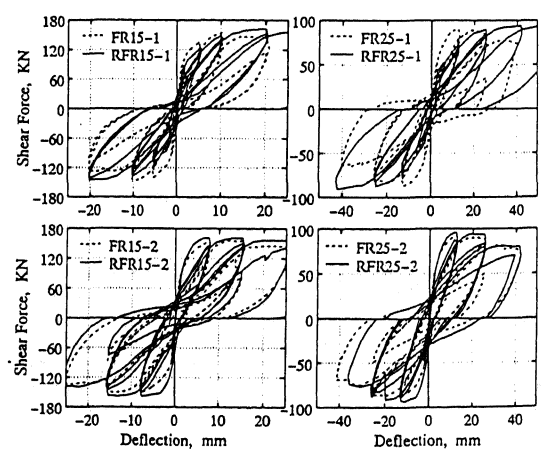

Fig.4 Restoring Force Characteristics

dinal round bars.

When subjected to larger deformation than 1/50 rad in deflection angle, no deterioration was observed in resistance of specimens RFR15-1 and RFR25-1; crushed regions were repaired with high strength material. The resistance of specimens RFR15-2 and RFR25-2 degraded in the same manner as the original loading probably because the material properties of prepacked concrete in the repaired critical regions was almost similar to that of the normal concrete.

2.4 *Recovery of Bond*

Stress distributions along the longitudinal reinforcement during the load reversal at 1/100 rad in deflection angle are shown in Fig.5. Since the strain along the longitudinal reinforcement located at mid-span did not exceed the yield strain, stress in the steel was estimated from measured strain by assuming a linear relation. Solid and dashed lines differentiate loading directions. No bond was observed in specimens FR15-1 and FR25-1 (Fig.5.c,d). In specimen FR15-2, high bond was observed within the clear height (Fig.5.e). In specimen FR15-2, sudden change in stress distribution was observed in the part where the cover concrete was replaced by epoxy resin as illustrated in the meshed part in Fig.5.f, that represents high bond strength of epoxy mortar.

Thus, the both bond repair methods, using prepacked concrete for the short column and epoxy mortar for the long column, were effective to restore the bond performance of the longitudinal round bar. Observed bond strength of repair material is shown in Fig.6.

2.5 *Bond Repair Length in the Mid-span*

A resisting mechanism to external forces in specimen RFR25-2 was considered based on truss analogy (Fig.7). Permitting no crack in the mid-span, tension resultant T_c must be carried by the concrete.

Bond repair length L_R is expressed as follows.

$$L_R = (T_s + C_s)/(\tau_d \cdot \psi \cdot n) \quad (1)$$

where, τ_d = bond strength between repair material and a main bar, ψ = perimeter of a main bar, and n = number of main bars in one layer.

Assuming that tensile stress σ_t in concrete due to T_c occurs in the region within the bond repair length L_R and ignoring the effect of stress concentration, σ_t is expressed as the following equation.

$$\sigma_t = T_c/L_R \cdot B = (T_s + C_s) \cdot \tan\theta/(L_R \cdot B) = \tau_d \cdot \psi \cdot n \cdot \tan\theta/B \quad (2)$$

where, B = width of column.

Assuming that the condition of no cracking in concrete is $\sigma_t < \sigma_B/10$ (where σ_B is compressive strength of concrete), the following relation is derived from equation (2).

$$\tau_d < (\sigma_B/20)\sqrt{B/(\pi \cdot D \cdot n \cdot p_t)}\cot\theta \quad (3)$$

where, D = depth of column and p_t= ratio of tensile reinforcement.

Bond length is able to be decided by equations (1),(3).

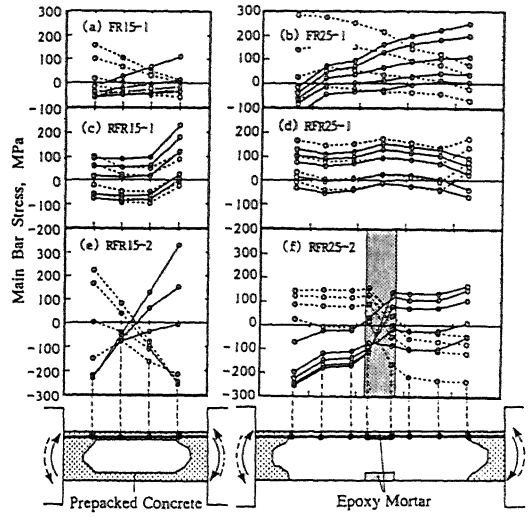

Fig.5 Main Bar Stress Distribution

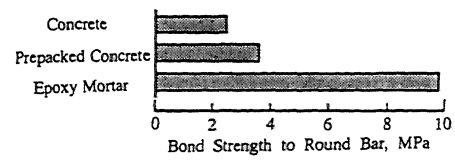

Fig.6 Bond Strength of Repair Materials

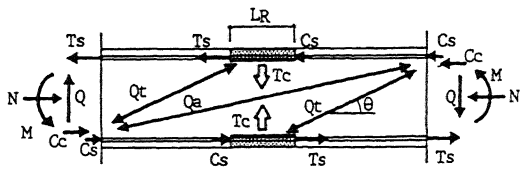

Fig.7 Resisting Mechanism of Mid-span Repair

3 REPAIR OF BOND ALONG DEFORMED BARS

The splitting bond failure of concrete columns reinforced with deformed bars was sometimes observed in strong earthquakes. This type of failure is often observed in the middle part of members with splitting of cover concrete along the longitudinal reinforcement.

Epoxy injection into the splitting cracks is an effective repair method for this type of failure. A test carried out at University of Tokyo is illustrated in Fig.8. The specimen had a uniform section of 250 x 250 mm with a 1000 mm clear height and reinforced by 5-D13 (nominal diameter: 13mm, deformed) in tension (Fig.8.a). Concrete had a compressive strength of 35.2 MPa and a tensile strength 3.2 MPa. The yield strength of main bar was 459 MPa. The specimen was subjected to antisymmetric bending reversals with no axial load. It failed in splitting bond failure with many cracks along main bars at under the original loading (Fig.8.b). After the original test, low viscous epoxy resin was injected so that the resin could penetrate into the splitting cracks. The repaired specimen did not develop any splitting cracks but failed in flexure during reloading (Fig.8.b). Load-deflection relations indicated that both

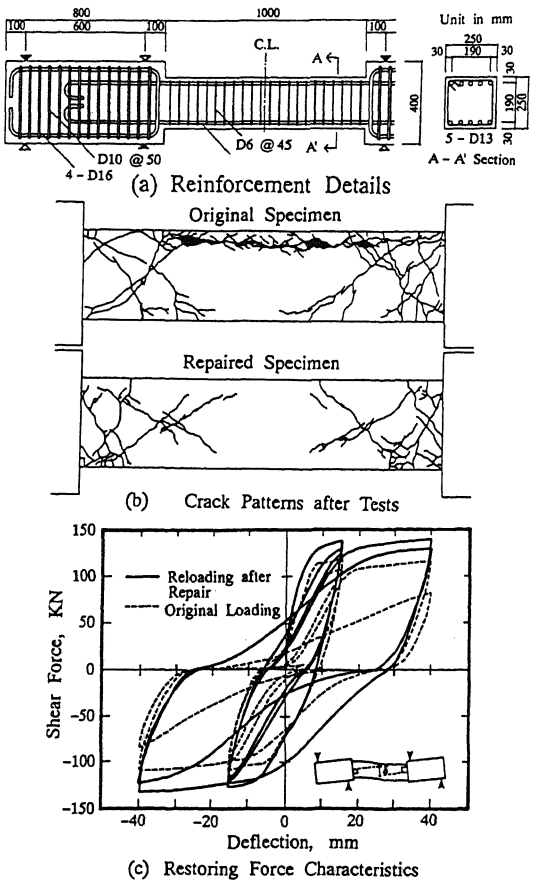

Fig.8 Effect of Epoxy Injection

stiffness and strength deteriorated considerably during original loading, while such deterioration was not observed after repair (Fig.8.c). Dissipated energy by the repaired specimen during last positive and negative loading exceeded twice that by the original specimen.

Thus, epoxy injection repair is effective to avoid splitting bond failure of repaired members. However, the bond strength after repair was unknown because the repaired specimen did not failed in bond. It is necessary to clarify how much the bond strength could increase by the repair in order to evaluate possible failure modes of repaired members. The following test series was conducted to clarify the level of bond strength after repair and the resisting mechanism.

3.1 *Outline of Test*

Three pull-out type specimens No1, No2 and No3 were tested. The specimens had the same dimensions and main bars (Fig.9). High strength D19 bars (nominal diameter: 19mm, deformed) were used to generate large bond stress even after repair. Anchorage length of main bars was 300 mm. Amount of lateral reinforcement was chosen as main variables (Table 2). Specimen No1 had no lateral reinforcement. Specimens No2 and No3 were laterally reinforced with 2-6ϕ(diameter

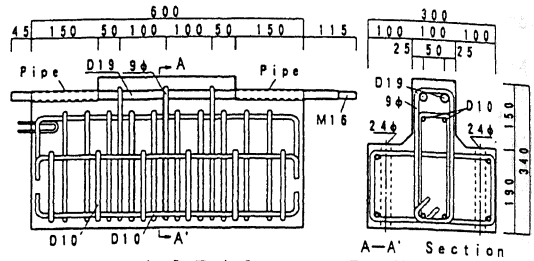

Fig.9 Reinforcement Details

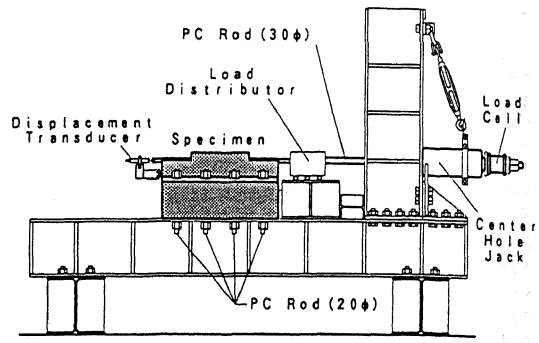

Fig.10 Loading Apparatus

Table 2 Variables of Specimens

Name of Original Specimen	NO1	NO2	NO3
Lateral Reinforcement	none	2-6ϕ@100	2-9ϕ@100
Main Bar	2-D19 (Common)		
Anchorage of Main Bar	300 mm (Common)		

Table 3 Material Properties (Unit: MPa)

(a) Concrete

Compressive Strength σ_B	26.1
Secant Modulus at $1/4\sigma_B$	19100
Split Tensile Strength	2.1

(b) Injected Epoxy Resin

Compressive Strength	74.2
Elastic Modulus	2650
Tensile Strength	44.0

(c) Reinforcement

	D19	6ϕ	9ϕ
Yield Strength	778	480	336
Elastic Modulus	189000	196000	207000
Tensile Strength	838	563	467

Note: Yield Strength of 6ϕ Bar is decided by 0.2% offset method.

6mm, round) and 2-9ϕ(diameter 9 mm, round) respectively at every 100 mm. Concrete was placed from the upper side of specimen. Main bars of original specimen were simultaneously pulled in one direction by a hydraulic center hole jack(Fig.10). Low viscous epoxy resin was injected into splitting cracks occurred during original loading. After the repair, main bars were pulled monotonically in the same manner as the original loading. Lateral displacement of main bars at their free ends were measured by displacement transducers. Distribution of elongation and curvature along lateral reinforcement were measured by strain gages. Material properties are listed in Table 3.

3.2 *Test results*

Crack patterns after tests are shown in Fig.11. All original specimens failed in bond splitting at the layer of main bars. In the repaired specimen No1R, no crack

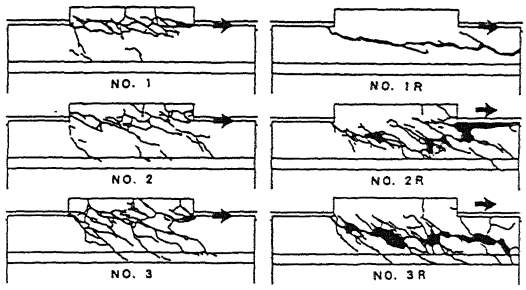

Fig.11 Crack Patterns

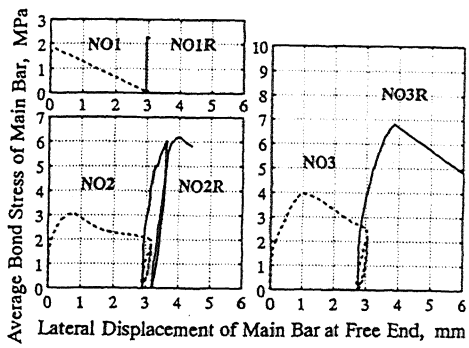

Fig.12 Bond Slip Relationship

along the layer of main bars was observed. This specimen failed suddenly in shear below the layer. In the repaired specimens No2R and No3R, some cracks were observed near the layer of main bars. However, these specimens also failed in shear below the layer.

Relations between average bond stress of main bars and lateral displacement at free end of main bar are shown in Fig.12. The relations after repair were plotted from the point of residual displacement. Stiffness in bond was completely restored by repair. Maximum bond stress of specimens No2R and No3R developed up to about twice that of original specimens.

3.3 *Stress of Lateral Reinforcement*

Distributions of average elongation and curvature along each lateral reinforcement were obtained from both tests before and after repair. Axial and shear forces distributions were calculated based on steel stress strain relationship obtained from a material test. Changes of the forces in lateral reinforcement of specimens No3 and No3R are plotted at every 1 MPa in average bond stress of main bars in Fig.13. The forces after repair are increments from residual forces due to original loading. Shear force distributions indicated dowel effect of lateral reinforcement. At the maximum resistance (at the maximum bond stress of main bars), both axial and shear forces in the original specimen were much higher than those in the repaired specimen. Therefore, contribution of lateral reinforcement to bond resistance of main bars was minor after repair.

3.4 *Bond Resisting Mechanism*

In the original specimen, adhesive action of concrete on

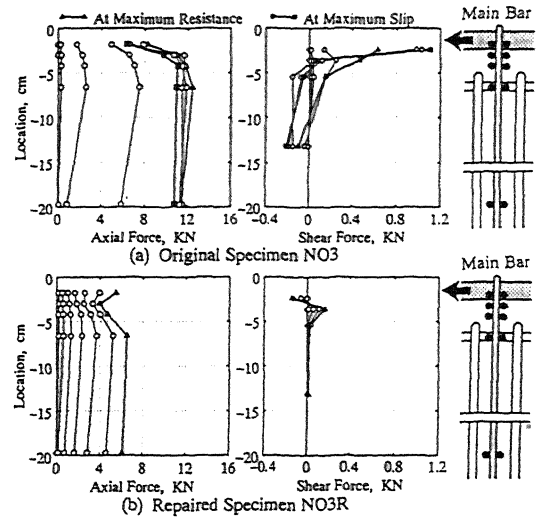

Fig.13 Stress of Lateral Reinforcement

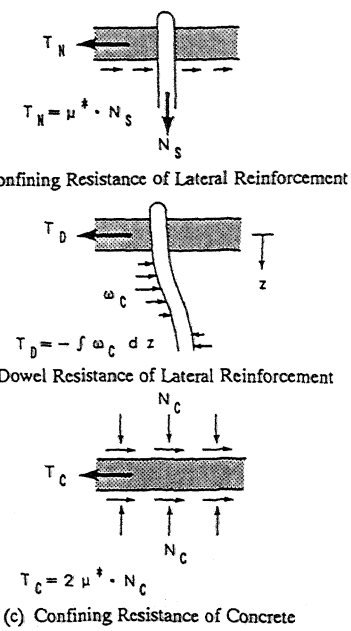

Fig.14 Bond Resisting Mechanism

the surface of deformed bars deteriorates at a low stress level. After the deterioration, possible bond resisting components are postulated as follows;

a) Friction resistance by confinement of lateral reinforcement: T_N

b) Dowel resistance of lateral reinforcement: T_D

c) Friction resistance by confinement of concrete: T_C

These resisting components are illustrated in Fig.14, where, μ^*: coefficient of friction between concrete and main bar defined in the axial direction of the bar, N_S: total axial force of lateral reinforcement, ω_c: distributed reaction force of concrete acting to lateral reinforcement, and N_C: confining force of concrete. Total tensile force T is represented as follows.

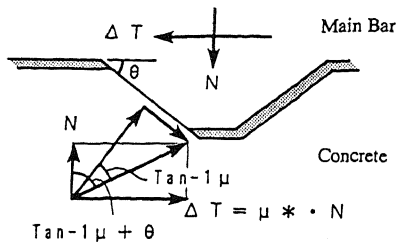

Fig.15 Resistance of a Rib

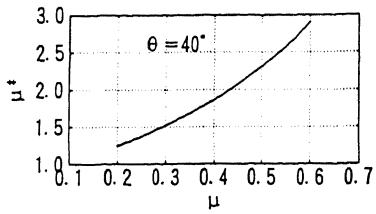

Fig.16 μ–μ^* Relationship

$$T = T_N + T_D + T_C \tag{4}$$

After the bond stress reaches the maximum, resisting components T_N and T_D will be dominant. The bond resistance of deformed bar was generated by friction between concrete and steel along the slope of ribs. Therefore, coefficient of friction μ^* is represented as the following equation (Fig.15).

$$\mu^* = \mathrm{Tan}(\,\mathrm{Tan}^{-1}\mu + \theta\,) \tag{5}$$

Where, μ: coefficient of friction between concrete and steel, θ: angle of rib's slope. The value of θ of D19 used in the test was about 40 degrees. Calculated μ–μ^* relationship is shown in Fig.16.

3.5 *Decomposition of Bond Resistance*

Confining force of lateral reinforcement N_S and dowel resistance of lateral reinforcement T_D of original specimens No2 and No3 were calculated at each loading step by summing up axial and shear forces of lateral reinforcement, respectively. Change in apparent coefficient of friction $(T-T_D)/N_S$ was studied as shown in Fig.17. Up to the maximum bond resistance, both effects of confinement to main bars by lateral reinforcement and by concrete were included in the apparent coefficient of friction. However, after the bond resistance reached the maximum, the apparent coefficient of friction represented only friction resistance by confinement of lateral reinforcement. The apparent coefficient was about 2.0 immediately after the maximum resistance (Fig.17). The value of μ^* was assumed to be 2.0. Resisting component T_N could be calculated using this value. Moreover, resisting component T_C could be determined by equation (4). The same resisting mechanism was assumed to exist also in repaired specimens.

The result of decomposition in specimens No3 and No3R is shown in Fig.18. In the original specimen No3, the maximum resistance was generated by T_N dominantly. On the other hand, in the repaired specimen

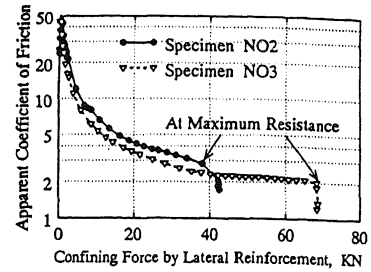

Fig.17 Apparent Coefficient of Friction

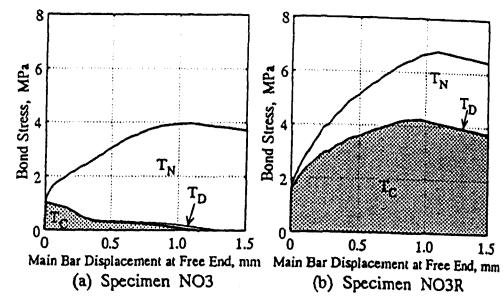

Fig.18 Decomposition of Bond Resistance

No3R, T_C contributed significantly to the maximum resistance. This fact means that the high bond strength of repaired specimens was developed by adhesive resistance of epoxy injected around main bars.

The dowel resisting by lateral reinforcement was considerably minor regardless of amount of reinforcement before and after repair.

4 CONCLUSIONS

In damaged members reinforced with round bars, repair of bond along main bars is necessary to restore the member stiffness. Bond repair using the prepacked concrete or epoxy mortar was so effective that the performance of repaired member was better than that of virgin member.

Epoxy injection into bond split cracks along deformed bars was an effective repair method to improve bond stiffness and strength. Bond strength after repair was more than twice that of original member. Decomposition into resisting components indicated friction resistance of main bars by confinement of concrete through injected epoxy layer increased drastically after repair.

Proposed repair methods make it possible to protect a repaired structure from bond failure. However, it is important to strengthen against other possible failure modes of the repaired structure.

ACKNOWLEDGMENTS

The author would like to express to Professor Hiroyuki Aoyama, Assistant Professor Shunsuke Otani, and the members of the Aoyama Laboratory, Department of Architecture, University of Tokyo, for their helpful advice and assistance in carrying out the study reported in this paper.